

0689

Dynamic Water/Fat Separation and Field Inhomogeneity Mapping at a Temporal Resolution of 40 ms

Zhengguo Tan¹, Dirk Voit¹, Jost M Kollmeier¹, Martin Uecker^{2,3}, and Jens Frahm^{1,3}

¹Biomedizinische NMR, Max-Planck-Institute for Biophysical Chemistry, Göttingen, Germany, ²Department of Diagnostic and Interventional Radiology, University Medical Center Göttingen, Göttingen, Germany, ³DZHK (German Center for Cardiovascular Research), Göttingen, Germany

Synopsis

To achieve dynamic water/fat separation even in the presence of rapid physiological motions and large magnetic field inhomogeneities, this work presents a multi-echo multi-spoke radial FLASH sequence and a model-based non-linear inverse reconstruction. Asymmetric echoes are integrated into the sequence to shorten echo times. A spatial-smoothness constraint on field inhomogeneity maps is developed to counteract local minima in the non-convex inverse problem.

Introduction

Water/fat separation based on proton water/fat chemical shift in multi-gradient-echo acquisitions^{1,2,3} has been of great interest in scientific research and clinical diagnostics. Due to the use of multiple echoes, however, it suffers from poor temporal resolution. Secondly, the successful separation of water and fat requires an accurate estimation of the B0 field inhomogeneity. Existing joint estimation techniques^{4,5} rely on proper initialization via region growing⁶, which is not applicable to dynamic imaging. To overcome these limitations, this work aims at developing: (1) an undersampled asymmetric-echo multi-echo radial FLASH sequence and (2) a model-based reconstruction technique with a spatial-smoothness regularization on B0 field map.

Methods

Figure 1 illustrates the multi-echo multi-spoke radial FLASH sequence and its corresponding k-space trajectory, where an echo asymmetry 75% is integrated to shorten TE and TR⁷. To achieve optimal coverage of k-space, radial spokes with the same TE are uniformly distributed in k-space, and the incremental angle between frames is empirically chosen as Golden angle (68.75°).

The signal model is:

$$F_{j,l}(x) = P_l \mathcal{F}\{(W + F \cdot z_l) \cdot e^{i2\pi f_{B0} TE_l c_j}\} \text{ with } x = (W, F, f_{B0}, c_1, \dots, c_N)^T$$

Here, P_l and \mathcal{F} are the sampling pattern for the l th echo and 2D FFT, respectively. The unknown x consists of water (W), fat (F), B0 field inhomogeneity (off-resonance) frequency (f_{B0}), and coil sensitivity maps (c_j). The fat modulation⁸ follows $z_l = \sum_{p=1}^6 a_p \cdot e^{i2\pi f_p TE_l}$. To jointly estimate all unknowns, the cost function is

$$\Phi(\hat{x}) = \operatorname{argmin}_{\hat{x}} \|y - F(T\hat{x})\|_2^2 + \alpha \|\hat{x}\|_2^2 \text{ with } x = T\hat{x}$$

y is the gridded k-space data without roll-off corrections. The weighting matrix is $T = \mathcal{F}^{-1} \left(1 + w \cdot \|\vec{k}\| \right)^{-h}$, with $w = 11$ and $h = 18$ for the B0 field map, $w = 880$ and $h = 16$ for coil sensitivity maps, while an identity matrix ($T = I$) is applied onto water and fat maps. \vec{k} is a 2D Cartesian grid matrix. Although weaker than coil sensitivity maps, the weighting on the B0 field map enforces spatial smoothness and assures accuracy. This cost function is minimized by the iteratively regularized Gauss-Newton method⁹ with automatic scaling¹⁰ for water and fat, while the scaling for the B0 field map is kept as 1.5 to warrant convergence. The reconstruction starts with $W = F = 1, f_{B0} = 0$, and $c_j = 0$, while the initialization for the following frames is set as the estimate from the preceding frame damped by 0.9 to enforce temporal continuity.

Data acquisitions were performed on a 3T scanner (Magnetom Prisma, Siemens Healthineers, Erlangen, Germany) with an 18-channel body matrix coil. Acquisition parameters were: 8° FA, standard shimming, 1560 Hz/Px bandwidth, 320 x 320 mm² FoV, 200 x 200 matrix size, 1.6 x 1.6 x 6 mm³ spatial resolution, and 40 ms temporal resolution with 9 RF excitations per frame and TR = 4.43 ms, TE = 1.26/2.66/3.69 ms.

In addition, a whole-body scan with the built-in 2-channel body receiver coil was conducted. The volunteer was pulled through the isocenter from the lower leg to the head. Acquisition parameters were: 16° FA, tune-up shimming, 1200 Hz/Px bandwidth, 448 x 448 mm² FoV, 320 x 320 matrix size, 1.4 x 1.4 x 10 mm³ spatial resolution, and 50 ms temporal resolution with 9 RF excitations per frame and TR = 5.54 ms, TE = 1.54/3.12/4.70 ms. This scan covers the whole body within only 40 s. To accompany with rapid change of anatomies from slice to slice, a real non-negative constraint is applied on water and fat maps during image reconstructions.

Results

Figure 2 shows results of a static phantom using the proposed acquisition and joint estimation techniques. The reconstruction is able to capture fast varying B0 field inhomogeneity across the FoV. Moreover, temporal B0 field inhomogeneity variations in the presence of abdominal breathing are well resolved (see Figure 3). When imaging the beating heart, the proposed method again accurately separates water and fat in different sections and for all cardiac phases (see Figure 4). In the experiment where the volunteer was pulled through the isocenter, the field inhomogeneity changes rapidly along with anatomy, as depicted by the selected slices in Figure 5.

Discussion and Conclusion

B0 field homogeneity is affected by various factors, e.g., shimming, tissue composition, and motions. Therefore, accurate estimation of dynamic field inhomogeneity maps is crucial for the successful separation of water and fat. The proposed sequence and joint estimation reconstruction provide a practical solution to time-resolved water/fat separation at a temporal resolution of 40 ms.

Acknowledgements

The authors would like to thank Dr. Arun Joseph, Olkesandr Kalentev, Klaus-Dietmar Merboldt, and Thomas Michaelis for their help on the experiments.

References

1. Dixon WT. Simple proton spectroscopic imaging. *Radiology* 1984;153:189-194.
2. Glover GH. Multipoint Dixon technique for water and fat proton and susceptibility imaging. *J Magn Reson Imaging* 1991;1:521-530.
3. Reeder SB, Wen Z, Yu H, et al. Multicoil Dixon chemical species separation with an iterative least-squares estimation method. *Magn Reson Med* 2004;51:35-45.
4. Doneva M, Börnert P, Eggers H, et al. Compressed sensing for chemical shift-based water-fat separation. *Magn Reson Med* 2010;64:1749-1759.
5. Benkert T, Feng L, Sodickson DK, et al. Free-breathing volumetric fat/water separation by combining radial sampling, compressed sensing, and parallel imaging. *Magn Reson Med* 2017;78:565-576.
6. Berglund J, Johansson L, Ahlström H, et al. Three-point Dixon method enables whole-body water and fat imaging of obese subjects. *Magn Reson Med* 2010;63:1659-1668.
7. Untenberger M, Tan Z, Voit D, et al. Advances in real-time phase-contrast flow MRI using asymmetric radial gradient echoes. *Magn Reson Med* 2016;75:1901-1908.
8. Hu HH, Börnert P, Hernando D, et al. ISMRM workshop on fat-water separation: Insights, applications and progress in MRI. *Magn Reson Med* 2012;68:378-388.
9. Uecker M, Hohage T, Block KT, et al. Image reconstruction by regularized nonlinear inversion – Joint estimation of coil sensitivities and image content. *Magn Reson Med* 2008;60:674-682.
10. Tan Z, Hohage T, Kalentev O, et al. An eigenvalue approach for the automatic scaling of unknowns in model-based reconstructions: Application to real-time phase-contrast flow MRI. *NMR Biomed* 2017;30:e3835.

Figures

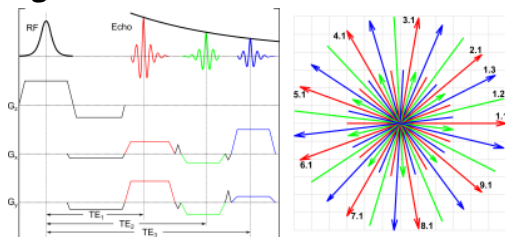


Figure 1. Multi-echo multi-spoke radial FLASH with asymmetry of 75 % (left) and the corresponding k-space trajectory (right), where a total of 27 spokes are acquired via 9 RF excitations with 3 echoes per excitation. Blip gradients (dark triangle) are used to connect two neighboring echoes with different radial spokes. The index $k.l$ denotes the l th echo in the k th excitation.

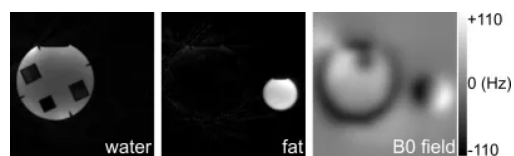


Figure 2. Reconstructed water (left), fat (center), and B0 field inhomogeneity frequency (right) maps of a static phantom, which consists of the Siemens structure phantom and a bottle of cooking oil (92% fat per 100 mL).

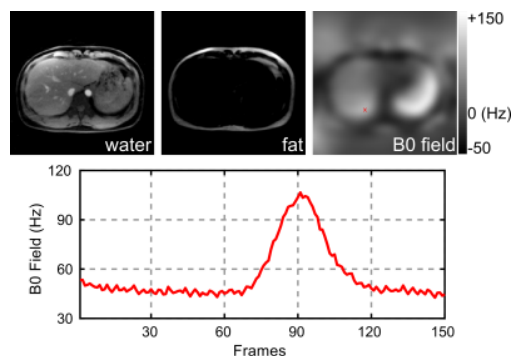


Figure 3. Reconstructed water (upper left), fat (upper center), and B0 field inhomogeneity frequency (upper right) maps of a transversal abdomen slice. A B0 field temporal line profile through the red dot is plotted at the bottom. B0 field homogeneity is perturbed by breathing.

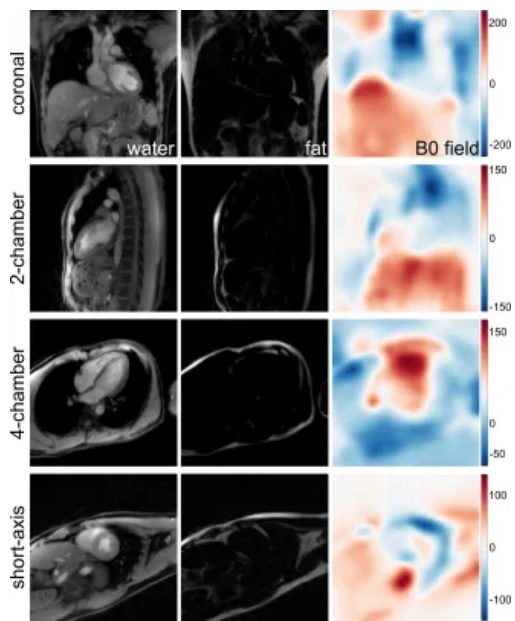


Figure 4. Representative water (left), fat (center), and B0 field inhomogeneity frequency (right) maps of human hearts from the proposed acquisition and reconstruction methods. Imaging slices from top to bottom are coronal, 2-chamber, 4-chamber, and short-axis, respectively.

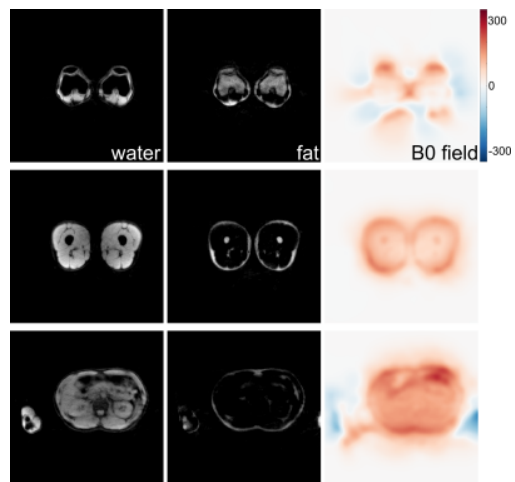


Figure 5. Reconstructed water (left), fat (center), and B0 field inhomogeneity (right) maps from the whole-body scan. Selected slices from top to bottom are knee, thigh, and kidney, respectively. As the volunteer was pulled through the isocenter, severe field inhomogeneity occurs at later slices.